Available online at www.sciencedirect.com
SCIENCE DIRECT®
Applied Catalysis A: General 278 (2004) 11–23
APPLIED CATALYSIS A: GENERAL
www.elsevier.com/locate/apcata

Catalytic activity of the M/(3ZnO·ZrO_2) system (M = Cu, Ag, Au) in the hydrogenation of CO_2 to methanol

J. Słoczyński[a,*], R. Grabowski[a], A. Kozłowska[a], P. Olszewski[a], J. Stoch[a], J. Skrzypek[b], M. Lachowska[b]

[a]*Institute of Catalysis and Surface Chemistry, Polish Academy of Sciences, Niezapominajek 8 Str., Kraków 30239, Poland*
[b]*Institute of Chemical Engineering, Polish Academy of Sciences, Gliwice, Poland.*

Received 10 May 2004; received in revised form 26 July 2004; accepted 6 September 2004

Abstract

Morphology, surface composition, dispersion of the metals were determined for a series of the M/(3ZnO·ZrO_2) catalysts (M = Cu, Ag, Au) with the use of the XPS, XRD and TEM techniques. Catalytic activity in the reaction of the synthesis of methanol from CO_2 was also determined. The catalysts contain crystallites of ZnO and amorphous ZrO_2, and they show a considerable segregation of the components. The surface is depleted of the metal, metallic Cu is present mainly in the surrounding of ZnO. In the catalysts containing gold and silver, Au and Ag are distributed more uniformly. The dispersion of the metals in the catalysts depends on the nature of the metal and decreases in the series Au ≅ Cu > Ag, and for a given metal it decreases with the increase in the metal content. The catalysts containing copper exhibit by far higher catalytic activity when compared to the catalysts containing Ag and Au, due to a synergy between Cu and ZnO or ZrO_2.

Keywords: Methanol synthesis; CO_2 hydrogenation; Noble metals catalysts

1. Introduction

Synthesis of methanol from CO_2 has gained an increasing interest in the last decade [1,2], since it allows a reduction of the greenhouse effect. On the other hand, CO_2 may be regenerated in the hydrogenation – steam conversion cycle, and hydrogen produced can be used in fuel cells [3–5]. High activity, in CO_2 hydrogenation, of the catalysts containing Cu and zirconia has been well documented [6–10]. Activity, in the process, of the catalysts containing silver [11–15] or gold [11,12,15–19] has been also reported. Recently Sakahara et al. [20] have demonstrated, using methods of quantum chemistry, that silver and gold in the cationic form (Ag^+, Au^+) should be active in the methanol synthesis.

Data concerning the catalytic activity of the two latter systems are scarce and contradictory, no comparison of the results obtained with those for the standard copper catalysts of known activity is either available. A quantitative comparison of the results of various authors obtained for catalysts containing various metals is of little value since the catalysts were prepared in various ways and the catalytic tests were carried out under conditions markedly differing between each other.

The aim of the present work has been a verification of the results obtained so far by determining the catalytic activity in the reaction of the methanol synthesis from CO_2, for a series of catalysts containing Cu, Ag, Au of varying metal content, obtained and investigated according to a uniform methodology. Relationships between structure of the catalysts and their catalytic activity were also studied.

The selected composition of the support, 3ZnO·ZrO_2, is optimal according to Nitta et al. [21] who investigated the catalytic activity in the synthesis of methanol from CO_2 for a series of Cu/ZnO/ZrO_2 catalysts of varying contents of ZrO_2 and ZnO. The selected composition corresponds also to

* Corresponding author. Tel.: +48 12 63 95 160; fax: +48 12 425 19 23.
E-mail address: ncgrabow@cyf-kr.edu.pl (R. Grabowski).

0926-860X/$ – see front matter © 2004 Elsevier B.V. All rights reserved.
doi:10.1016/j.apcata.2004.09.014

formulations of the Cu/ZnO/ZrO_2 catalysts recommended for practical applications as highly active catalysts for the synthesis of methanol from CO_2 [22–24].

2. Experimental

Preparation method: Oxide precursors of the M/ZnO/ZrO_2 catalysts (M = Cu, Ag, Au), in which the mole ratio ZnO/ZrO_2 = 3 was kept constant, and the metal contents were 2, 10 and 62.5 at.% were obtained by co-precipitation and calcination of the precipitate of mixed basic carbonates. Content of metals was expressed as percent of the total metal content − sum of metals was taken as 100%. The following reagents were used to introduce zirconium: (a) 30 wt.% solution of $ZrOCl_2$ in hydrochloric acid from Aldrich, which contained the following contaminants: about 200 ppm Ca, heavy metals (Fe, Co, Ni, Pb) in quantities not exceeding 50 ppm each, as well as Na and K at the order of 5 ppm. The presence of P and S was not found, (b) technical $ZrO(NO_3)_2$ sol from Mel Chemicals (UK) containing around 30 wt.% ZrO_2 + 0.6 wt.% HfO_2, which differed from (a) by a higher content of Ca (480 ppm) and Na (1660 ppm), (c) solid $ZrO(NO_3)_2{\cdot}H_2O$ (Aldrich 99.99%). It was found that the structure of the precursors and the activity of the catalysts did not depend on the nature of the reagents used to introduce ZrO_2. Solution (a) was used in preparation of the catalysts containing Cu and Au, and solution (b) for the Ag catalysts. The remaining metals were introduced by using nitrates of Zn, Cu, Ag and $HAuCl_4$ from Aldrich of 99.99% purity. The solution containing Zr, Zn and a given metal M, as well as 0.25 mol/l solution of Na_2CO_3, were simultaneously added to a vessel containing demineralised water under vigorous stirring. The precipitation was carried out at the temperature of 338 K and a constant pH = 7. The precipitate aged in the mother solution for 24 h at same temperature under stirring and then was washed many times with demineralised water (until disappearance of Na^+, Cl^- or NO_3^- in the solution), dried for 3 h at 383 K and calcined for 3 h at 623 K on air. The XPS analysis showed no presence of Na or Cl in the obtained catalysts. Prior to the XRD investigations and the measurement of the active Cu surface, the precursors containing copper were reduced in situ at 523 K in the stream of the 5 vol.% H_2 in Ar. High purity gases from BOC Gases (UK) were used in which sum of the impurities did not exceed 10 ppm.

The specific surface area and pore size distributions of the oxide precursors and of the reduced catalysts were determined with the BET and BJH methods using an Autosorb-1 Quantachrome apparatus with nitrogen as adsorbate at 77.5 K. ChemBet-3000 Quantachrome was used for the reduction of the catalyst samples in situ to determine the specific surface area of the reduced catalysts.

The phase compositions of the oxide precursors were determined with a Bruker/AXS diffractometer, Cu Kα radiation and graphite monochromator. The reduction of the precursors was carried out in a high temperature camera XRK-900 Anton Pear, with a gas flow (5 vol.% H_2 in N_2, 40 cm^3/min). The sample was rotated in order to minimize textural effects. CuO(1 1 1) and Cu(1 1 1), Ag, Au diffraction maxima were monitored to observe a progress of the reduction. Diffractograms were recorded in a range between 25° and 58° (2θ) at a scanning rate of 0.02°/s at temperatures of 298, 523, 623, 773 K when the stationary values were reached. Slow scanning of the selected peaks was carried out to determine the mean size of metal M particles. The quantitative phase contents, and crystal size of metal M were determined by a multiphase Rietveld refinement using Topas (Bruker AXS, Germany, 2000) software and a fundamental parameters approach for modeling of peak shape.

Morphology and structure of the catalysts was investigated by the transmission electron microscopy (TEM), electron diffraction (ED) using a Philips CM-20 electron microscope at the voltage of 200 kV. The selected area diffraction (SAD) technique was used for the ED measurements. Elemental compositions of the samples were determined using an EDX microanalyser. The probe size used for EDX was 10 nm and the energy beam range 0.3–40 keV. Ground samples were deposited from the suspension in ethanol onto the carbon film and placed on an aluminum or copper grid.

The active surface of copper in the reduced catalysts was determined with the use of the reactive adsorption of N_2O at 363 K according to the method described in [25]. The measurements were carried out in a flow micro-reactor of stainless steel—length 18 cm, i.d. 1.3 cm. Approximately 0.5 g of a catalyst was reduced at 523 K during 3 h and cooled to 363 K. Then 100 μl of N_2O pulses were injected until the reaction was completed. Amount of the reacted N_2O was determined using a mass spectrometer (VG/Fisons Quartz 200 D). It has been assumed in the calculations that the reoxidation of the surface copper follows the equation:

$$2Cu_{(s)} + N_2O_{(g)} = Cu_2O_{(s)} + N_2 \quad (1)$$

and 1 m^2 of elemental copper corresponds to 6.1 μmol O_2.

XPS spectra of the catalysts were obtained with a VG ESCA-3 spectrometer equipped with an aluminium anode (Al Kα = 1486.6 eV) at a power of 240 W (12 kV and 20 mA). The pass energy of the analyser was set at 50 eV. An energy step width of 100 meV and a dwell time of 100 ms were chosen. Thirty scans were accumulated for each spectrum. The powder samples for the XPS measurements were placed on standard VG sample stubs by the settling from a suspension. Before recording spectra, the samples were stored to degas overnight at a pressure $<10^{-8}$ kPa in the preparation chamber. Pressure within the spectrometer chamber during the measurements was less than 10^{-6} kPa. Samples containing CuO were reduced in situ in the chamber of the spectrometer at 573 K under hydrogen at the atmospheric pressure. In addition to samples of the catalysts, simple compounds: Cu_2O, CuO, ZnO and ZrO_2 were examined to get parameters for the spectra analysis. The

band structure (number of constituent peaks, $2p_{3/2}$–$2p_{1/2}$ distance and their height ratio) used was the same as in the pure, simple compounds. In the case of Cu(II) also the satellite was taken into account. During processing of the XPS spectra, binding energy (BE) values were referenced to the C 1s peak (284.8 eV) from adventitious contamination layer, background of Shirley's type and $K\alpha_{3/4}$ peaks were removed and resulted spectra were fitted with symmetric single peaks or doublets. The error in the binding energy was estimated to be ±0.1 eV. All XPS bands, i.e. C 1s, O 1s, Zr 3d, Zn 2p, Cu 2p and Auger bands CuKLL and ZnKLL were fitted using a Voigt function with 30% Lorenzian character. The relative element content (N) was calculated using formula (2) according to [26]:

$$N = FI_A E_A^{0.25} \sigma_A^{-1} \exp(d_C \lambda_{A,C}^{-1}) \quad (2)$$

where F contains all instrumental factors (including transmission function T) and is assumed to be constant for the measurements, I_A the intensity of the line A measured, E_A the kinetic energy of the A-level, σ_A the elemental cross-section for photo ionization, $\lambda_{A,C}$ the A-level electrons' inelastic mean free path in the adventitious carbon deposit and d_C is the thickness of the carbon deposit [27]. The λ and T values were obtained using the Penn approximation [27]. In this study, the empirically derived atomic sensitivity factors [28] were applied instead of σ_A in the element content calculations.

The catalytic activity was measured using a tubular, flow, high-pressure, fixed-bed reactor of volume 8 cm^3, made of stainless steel. The bed consisted of 2 g of the catalyst placed between two layers of ceramic grains (porcelain). The catalyst was reduced in a stream of diluted hydrogen (10 vol.% H_2 in N_2) at 473 K under atmospheric pressure for 15 h and activated in the mixture of the reactants by raising the temperature by steps of 30° between 473 and 623 K every 2 h. Preliminary experiments have shown that during the heating of the catalyst between 473 and 623 K the specific activity first increases and then decreases. The increase in the activity reflects the desorption of water from the catalyst surface and unblocking the active centres, whereas the decrease of the activity observed at higher temperatures results from the sintering of the catalysts and the agglomeration of the dispersed metal, which was formed during the reduction of the catalyst at 473 K. The catalysts, which were subjected to the thermal treatment described above, show a constant activity within the temperature range between 453 and 523 K. The catalytic activity in the methanol synthesis was determined under the following conditions: pressure 8 MPa, temperature range 453–523 K, space velocity of the reactants flow GHSV 1000–10 000 h^{-1}, composition of the reactant mixture $H_2/CO_2 = 3$. The feed gas was deoxidised with the BTS deoxidizer and dehydrated with the molecular sieve 5A. After leaving the reactor, the gases were decompressed to the atmospheric pressure and the reaction products were analysed chromatographically with Varian Star 3600 and Star 3800 chromatographs. Methanol was determined with a Suplowax column, a FID detector and a Carbosieve column, and a TCD detector for other gaseous product was used. Hydrocarbons were detected by a GS alumina column (FID). It has been checked in the preliminary experiments, in which the mass and the grain size of the catalyst were varied, that under these conditions the transport phenomena do not limit the reaction rate. Catalytic activity is presented as stationary values, established after 10–20 days.

3. Results and discussion

3.1. Surface area and porosity structure

Results collected in Table 1 show that surface area of the oxide precursors decreases with an increasing content of metal M. The decrease in the surface area is the smallest for the copper catalysts and the most significant for the catalysts containing silver. After the activation of the catalysts at 623 K, and the catalytic tests, the surface area always decreases.

Fig. 1 shows curves of the pore size distributions calculated according to the BJH procedure for the

Table 1
Characterization of the catalysts M/(3ZnO·ZrO_2)

M	Average M content[a] (at.%)	Surface area ($m^2\ g^{-1}$)		Crystal size of metal particles (nm)	Metal surface area from N_2O decomposition (m^2 (g M)$^{-1}$)
		Oxide precursor	Catalyst after test		
Cu	2	100	76	5.0	101
	10	101	64	9.8	55.5
	62.5	89	39	13.6	28.4
Ag	2	70	57	10.0	–
	10	41	30	24.5	–
	62.5	19	15	43.0	–
Au	2	76	59	2.5	–
	10	81	67	3.4	–
	62.5	50	25	26.0 (41)[b]	–

[a] As percent of total metals – sum of metals is 100%.
[b] 40 wt.% as Au metal + 60 wt.% as Au_3Zn. Crystal size of Au_3Zn is given in the parentheses.

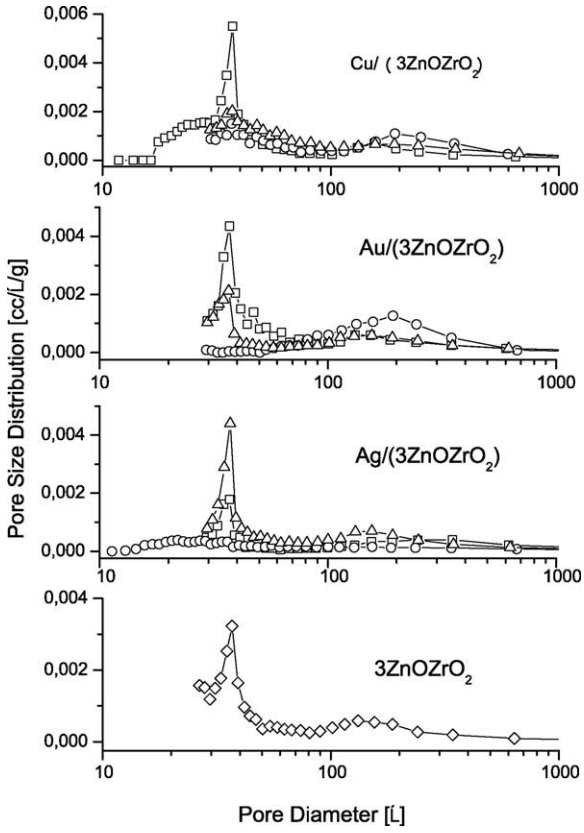

Fig. 1. Pore size distribution according to the pore width for M/(3ZnO·ZrO_2) precursors: (◇) 0 at.% M; (△) 2 at.% M; (□) 10 at.% M; (○) 62.5 at.% M.

investigated catalysts and the support. As one can see, both the support and oxide precursors contain mesopores of the diameters of 35 and 150–200 Å, the latter correspond most probably to the intercrystalline spaces.

For the copper catalysts, introducing very small amounts of CuO reduces the number of the pores of 35 Å diameter, and the 10 at.% addition of CuO brings about a marked increase in the population of the pores of that diameter. Introducing large amounts of CuO (62.5 at.%) leads practically to a disappearance of the 35 Å mesopores and to a formation of pores of the diameter of about 200 Å which are probably related to the crystallization of CuO. A similar situation is observed for the precursors containing Au. In the case of the Ag containing samples, the number of pores decreases monotonically with increasing Ag loading. The precursor containing 62.5 at.% Ag is an exception since very large Ag crystallites formed in this case eliminate the porous structure.

The comparison of the porosity before and after the catalytic tests indicates that a long-term influence of the reductive conditions brings about crystallization of the components of the catalyst and disappearance of the intercrystalline spaces, probably due to the sintering of the catalyst.

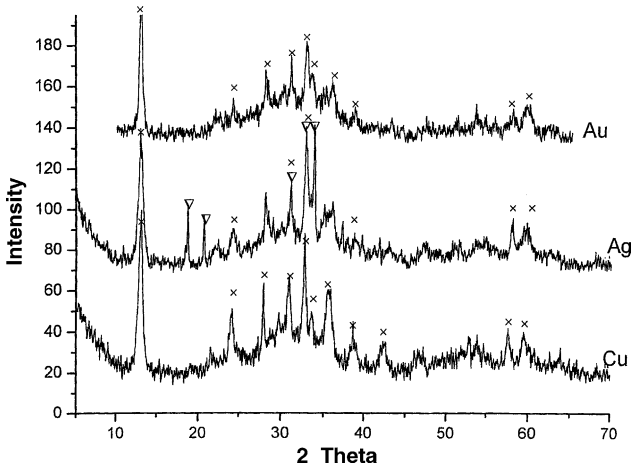

Fig. 2. XRD patterns for the coprecipitated precursors of the catalysts M/(3ZnO·ZrO_2) containing 10 at.% of metal M, where M = Cu, Ag, Au; *x*-hydrozincite $Zn_5(OH)_6(CO_3)_2$ or $(Cu_{0.2}Zn_{0.8})_5(OH)_6(CO_3)_2$; (▽) Ag_2CO_3.

3.2. Phase composition and morphology of the precursors and the catalysts

Fig. 2 shows XRD patterns for the coprecipitated precursors dried at 383 K which contained 10 at.% of a metal M = Cu, Ag, Au. The figure clearly reveals that the precipitates dried at 383 K contained Zn, mixed ZnCu hydrozincite and silver carbonate. For large contents of Cu also malachite was detected.

It is evident from Fig. 3 that after a calcination at 623 K crystalline ZnO is present but crystallization of ZrO_2 is not observed. The crystallisation of this oxide occurs only after an additional heating till 773 K (tetragonal ZrO_2). In the precursors containing Ag or Au in the amounts $\geq$10 at.% presence of metallic forms was identified already after the calcination on air. CuO was present however in the copper precursors which oxide was undergoing at 473 K a fast reduction to metallic copper under hydrogen (mixture of 5 vol.% H_2 in N_2).

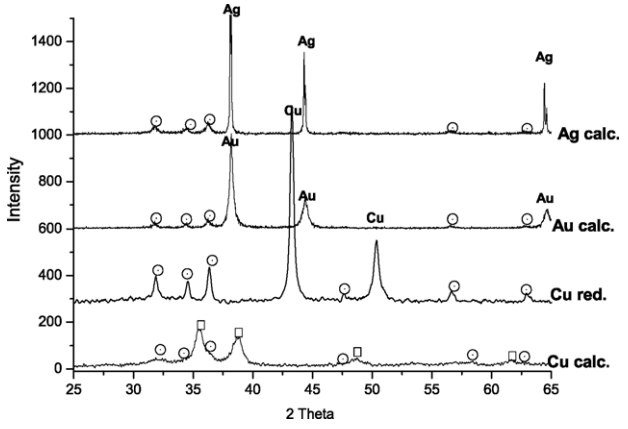

Fig. 3. XRD patterns for the precursors of the catalysts M/(3ZnO·ZrO_2) containing 62.5 at.% of M, where M = Cu, Ag, Au, calcined on air at 623 K. An XRD pattern after reduction for the copper catalyst was added; (⊙) ZnO; (□) CuO.

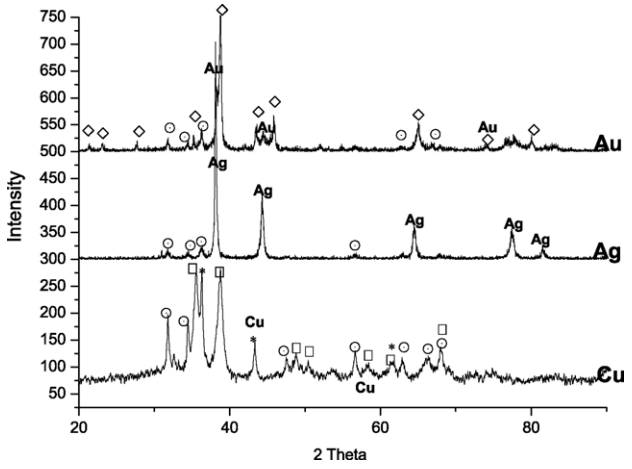

Fig. 4. XRD patterns for the catalysts M/(3ZnO·ZrO_2) containing 62.5 at.% of metal M, where M = Cu, Ag, Au, after reaction (10 days of work in the catalytic reactor); (○) ZnO; (□) CuO; (*) Cu_2O; (◇) Au_3Zn.

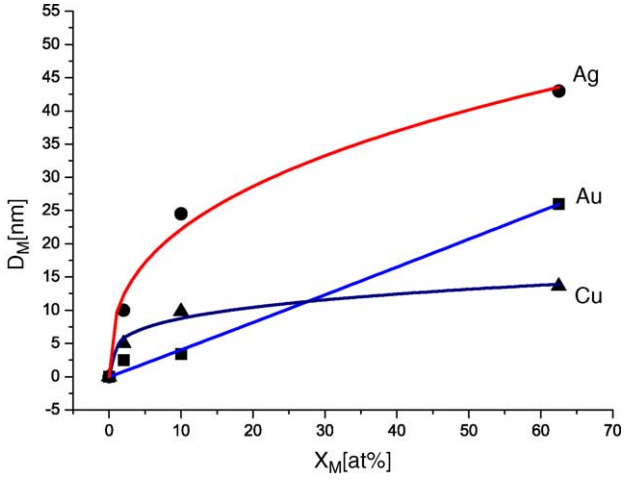

Fig. 5. Metal grain size as a function of the metal loading for the catalysts studied. Solid line was obtained using Eq. (4).

Fig. 4 illustrates phase changes which have occurred during 12 days of the catalyst's performance in a reactor. Intermetallic compound Au_3Zn of a specific structure [31], was formed in the catalyst containing Au. No phase changes were observed in the silver containing catalyst, merely a decrease in the width of the diffraction maxima, which evidenced a growth of the crystallites. Copper contained in the catalyst removed from the reactor underwent a partial reoxidation to CuO and Cu_2O.

Mean size of the metal crystallites determined with the XRD method for samples containing ≥10 at.% of metal M, after the catalytic reaction, are listed in Table 1. They agree with observations under a transmission microscope. Mean size of metallic grains for preparations containing 2 at.% M was assessed solely from the microscopic observations, since, due to a small content, the respective metals did not show any X-ray diffraction maxima. Table 1 shows that in all cases a systematic increase in the size of the metallic grains is observed with an increase in the metal content. This increase is the least significant for the copper catalysts and very abrupt for the catalysts containing Ag. In the copper catalysts, Cu preserves a relatively high dispersion in spite of high metal contents.

Fig. 5 shows the dependence between the size of the metallic grains (D_M) and the concentration of the metal X_M. It fits approximately the equation:

$$D_M^n = AX_M \tag{4}$$

where A is a constant, and exponent n is 4.0, 2.7 or 1.0 for Cu, Ag and Au, respectively. The above formula is derived from the equation commonly used to describe kinetics of sintering of metals on supports [29]:

$$\frac{1}{S^n} = \frac{1}{S_0^n} + kt \tag{5}$$

where S is the surface area of the metallic grains after sintering time t, S_0 the initial surface area of the metal, k a constant proportional to the metal concentration on the support, and the value of exponent n depends on the sintering mechanism. If S_0 is large enough $1/S_0^n$ may be neglected, and taking into account that $1/S$ is proportional to D, for constant t (Eq. (4)) is obtained. The value of $n = 2.7$ observed for Ag and 4.0 for Cu are typical of sintering limited by the surface diffusion. In contrast, lower values of $n = 1$ for gold indicate coalescence as a rate determining step. A similar dependence of the grain size on the metal concentration was observed by Bett et al. [30] during sintering of Pt on graphitized carbon black.

At high metal contents the grain size of metal increases in the order: Cu < Au < Ag. Such tendency is related to a markedly smaller binding energy of the metal in the structure of silver when compared to Cu and Au. According to Baker [32], temperature at which the structural mobility in the dispersed metals starts, is half of the bulk melting point ($0.5T_{mp}$ (K)). These temperatures are 678, 668 and 617 K, respectively, for Cu, Au and Ag. The values for copper and gold are close and significantly higher when compared to silver.

The microscopic observations, together with the microanalysis and the electron diffraction of selected areas allowed us to draw several conclusions on the morphology and distribution of components in the preparations

Table 2
Results of the EDX analysis of the M/(3ZnO·ZrO_2) catalysts, where M = Cu, Ag, Au

Catalyst	Elements (at.%)					
	Oxygen	Zinc	Zirconium	Copper	Silver	Gold
62.5 at.% Cu						
Amorphous area	10.8	16.0	38.0	35.3	–	–
Crystalline area	9.9	20.5	7.1	62.5	–	–
10 at.% Ag	2.2	3.5	2.5	–	91.8	–
10 at.% Au						
Amorphous area	25.9	17.5	38.8	–	–	17.7
Crystalline area	32.8	62.5	2.6	–	–	2.1

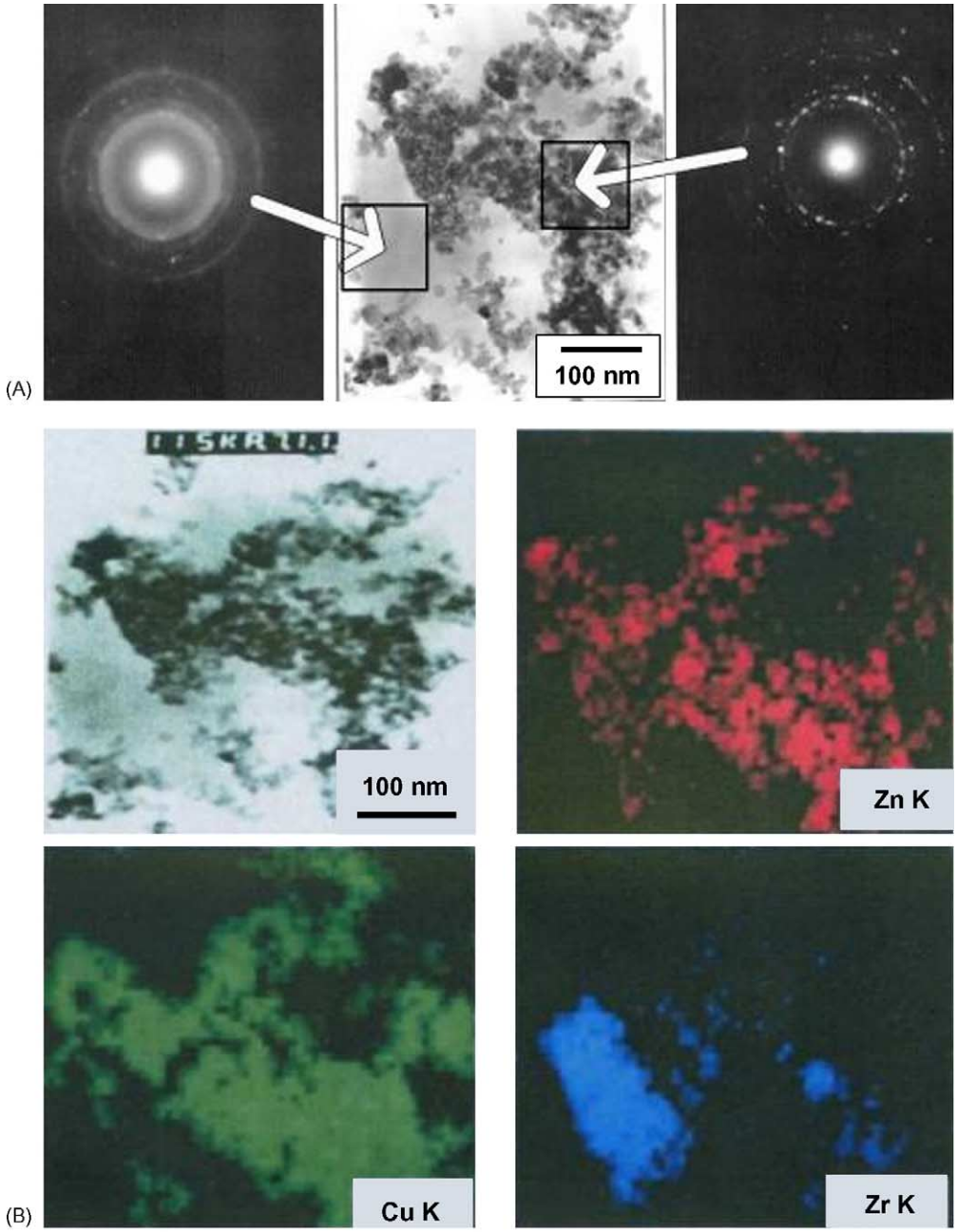

Fig. 6. (A) TEM/ED imaging for the catalyst containing 62.5 at.% Cu; (B) maps of the elements distribution for catalyst containing 62.5 at.% Cu.

investigated. Three kinds of areas are observed in all catalysts: areas containing mainly amorphous ZrO_2, areas in which crystalline ZnO dominates, and mixed areas. The situation is illustrated for the catalyst containing 62.5 at.% copper in Fig. 6A by showing the ED patterns for the areas described above. The positions of the diffracting spots for the crystalline area (right-hand side of Fig. 6A) correspond to the interplanar distances of ZnO, whereas the pattern of rings (left-hand side of Fig. 6A) points to the presence of an amorphous and microcrystalline phase. The EDX analysis of the above areas (Table 2) indicates that copper accumulates preferentially in the surroundings of crystalline ZnO. The same tendency for a broader area is shown in Fig. 6B presenting the distribution of the specific elements. One can clearly see that the distribution of zinc corresponds to that of copper.

For samples containing $\leq$10 at.% Au, two further kinds of areas are visible: the first enriched in crystalline ZnO and the other in which amorphous ZrO_2 dominates, which is illustrated in Fig. 7B. In this catalyst, gold accompanies preferentially amorphous ZrO_2 as revealed by the relevant EDX patterns and data in Table 2. The distribution of all components is more uniform in the sample containing 62.5 at.% Au as visible in Fig. 7A.

In the preparations containing silver, decisively larger metallic grains were observed when compared to Au and Cu

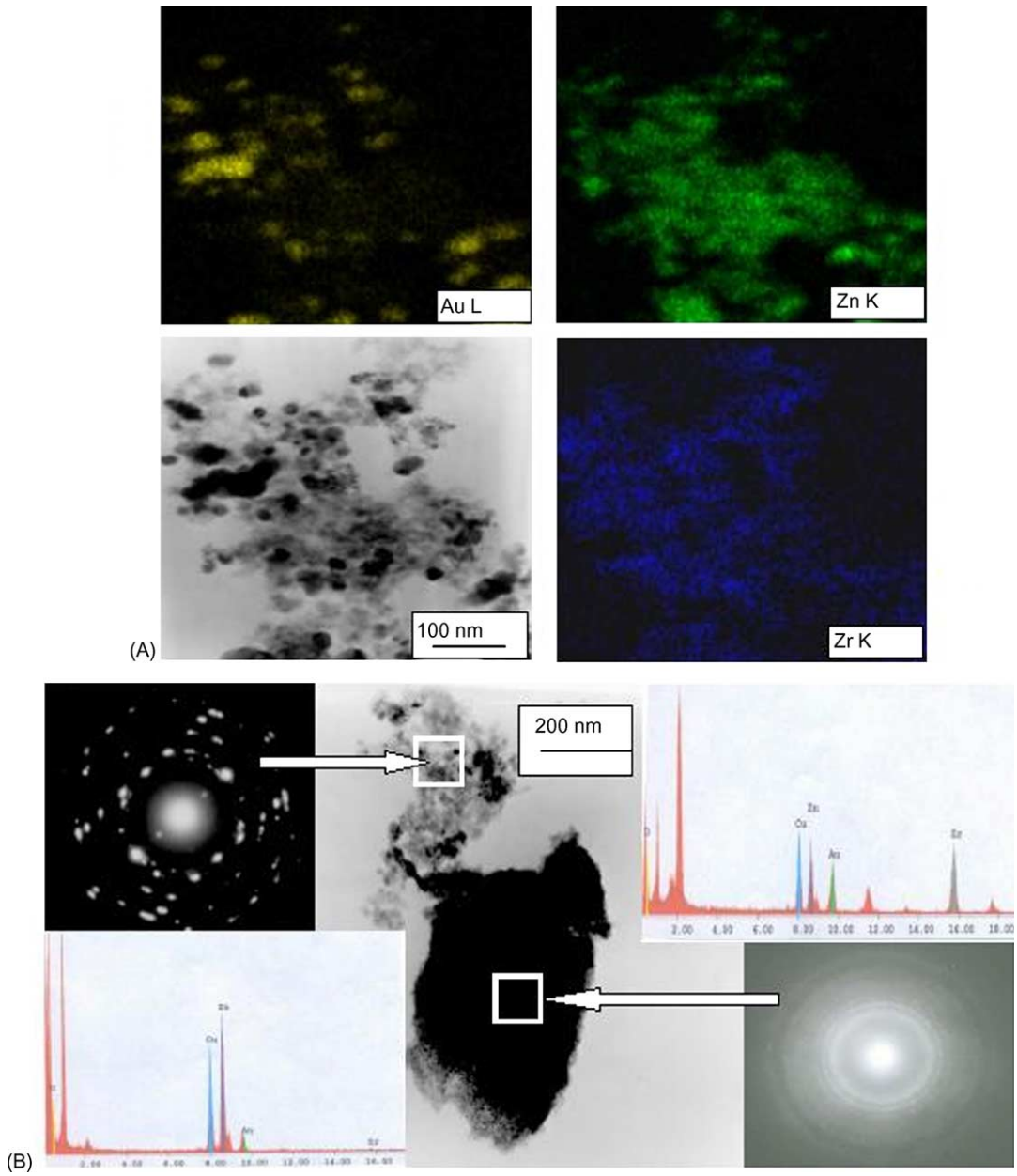

Fig. 7. (A) Maps of the elements distribution for catalyst containing 62.5 at.% Au; (B) TEM/ED imaging for the catalyst containing 10 at.% Au (copper peaks in EDX patterns come from a Cu grid used in the EDX measurements).

(Fig. 8B), as illustrated by the relevant EDX pattern of a selected grain of Ag and the numerical result given in Table 2. Large crystals of Ag are formed due to the segregation of silver already during the coprecipitation of the precursor, as evidenced by the presence of well-crystallised Ag_2CO_3. The silver grains show no preference to any component of the ZnO/ZrO_2 support and are randomly distributed in the entire volume of the catalyst, as shown in Fig. 8A.

3.3. Surface composition of the catalysts as determined with the XPS technique

In the XPS spectra of the reduced Cu catalyst, the BE of the Zr $3d_{5/2}$ band measured as 182.1–182.3 eV agrees within the error limit with the band position of ZrO_2 (182.2 eV). For zinc, the measured values of the kinetic energy of the Auger ZnKLL – 988.2–988.5 eV – also agree well with the ZnKLL band energy for ZnO (988.3 eV). Copper Cu(II) has the BE of the Cu $2p_{3/2}$ band above 933.5 eV which was absent on the reduced surface. Since the BE of the Cu $2p_{3/2}$ band in metal (932.67 eV) and in Cu_2O (932.4 eV) are almost the same, they can be distinguished by different kinetic energy of the Auger CuKLL line position in metal (918.65 eV), Cu_2O (916.8 eV) or in CuO (917.9 eV). Our data point to the metallic state of copper atoms, with possible polarization effects due to dispersion or short distance interactions with the supporting oxide matrix. In the Ag and Au catalysts the determined BE 367.7–386.0 and 83.4–84.0 eV agree well with the position of

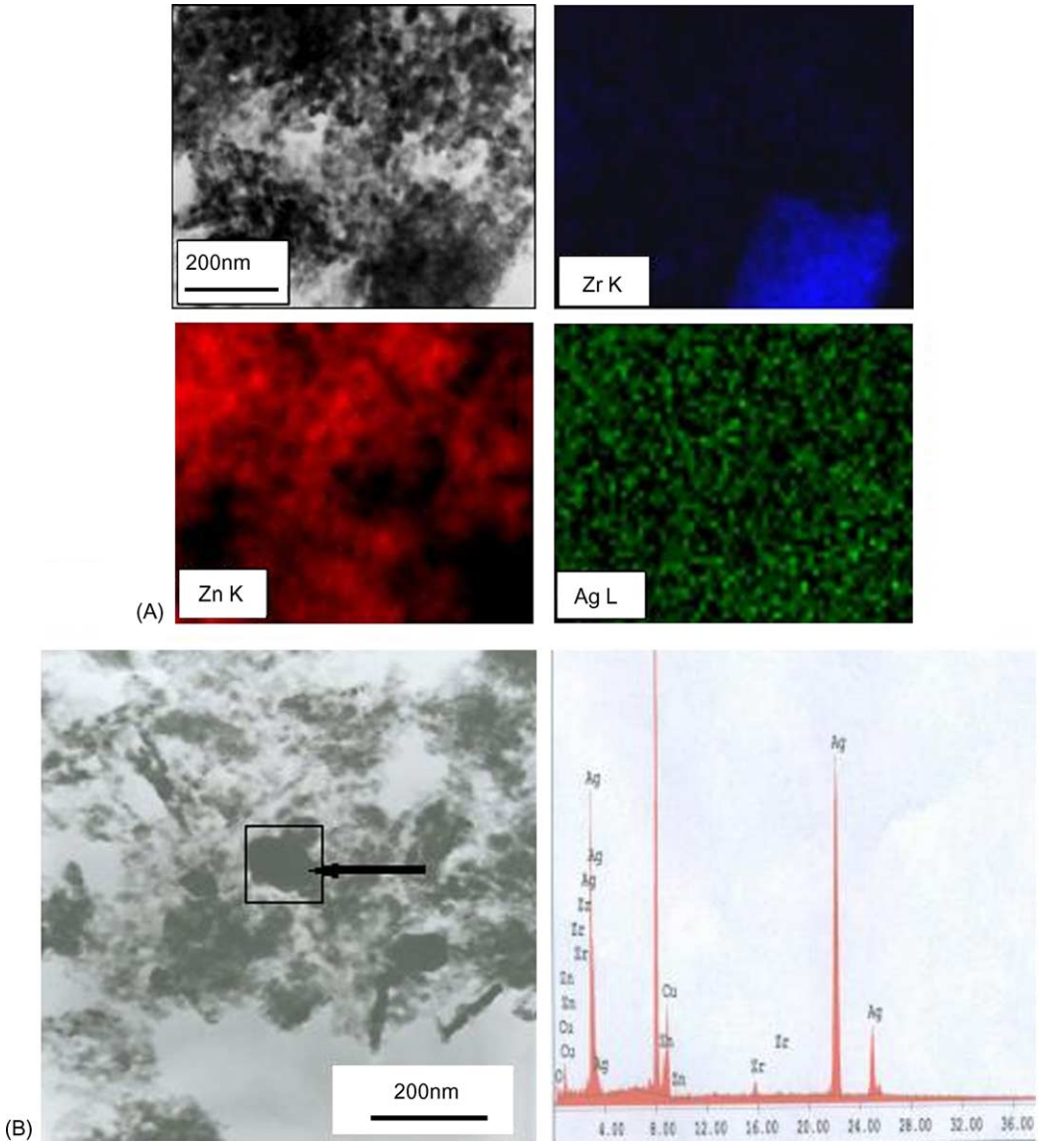

Fig. 8. (A) Maps of the elements distribution for the catalyst containing10 at.% Ag; (B) TEM micrograph for the 10 at.% Ag catalyst with the indication of the area used for the analysis (copper peaks in the EDX patterns come from a Cu grid used in the EDX measurements).

Ag 3d and Au 4f levels, respectively. A weak maximum of BE = 81.8 eV is visible only in the XPS spectrum for the preparation containing 62.5 at.% Au, which indicates that part of gold is present in a form different from pure metal. This result may provide an evidence that already at the stage of calcination a new phase containing Au is formed, the presence of which was identified by the X-ray diffraction analysis of the preparation after the catalytic reaction.

The oxygen O 1s could not been fitted with a single peak. Arbitrary decomposition into two components gives a more prominent peak at about 530.2 eV and the other at about 531.7 eV. The latter corresponds to a phase containing hydroxide and/or carbonate anions, whereas the former to the component of the oxide surface phase composed like ZrO_2 or ZnO.

Surface composition of the catalysts, as determined with the XPS method, is listed in Table 3. A ratio of the surface metal M content to the average value is also included. The last column of Table 3 contains ratio of the surface content of the metal $M_{surf} = M/(M + Zn + Zr)$ from XPS to the corresponding M_{av} listed in Table 1. The comparison shows that a far reaching segregation of the components occurs in the course of the catalyst preparation, i.e. during the precipitation, calcination and reduction. The surface is considerably depleted of Cu (four to seven times) in the reduced catalysts whereas in the oxide precursors the surface Cu^{2+} content is approximating the average value.

The oxygen content on the surface of the reduced copper catalysts is two times higher when compared to the stoichiometric composition calculated under assumption that only CuO has undergone the reduction to metal and that the remaining components are present as oxides (ZnO, ZrO_2). The extra oxygen on the surface is undoubtedly due

Table 3
Surface composition of the studied catalysts

M	Average M content[a] (at.%)	Surface composition (at.%)				M_{surf}/M_{av}
		M (metal)	Zn (ZnO)	Zr (ZrO_2)	Oxygen	
Cu	2	0.3	42.9	5.6	51.1	0.30 (0.80)
	10	2.1	38.7	7.3	51.9	0.44 (0.79)
	62.5	23.8	34.6	8.0	33.7	0.57 (0.98)
Ag	2	0.4	33.0	6.8	59.8	0.50
	10	1.1	33.9	5.1	59.9	0.26
	62.5	5.4	24.5	9.9	60.2	0.22
Au	2	0.7	37.1	3.4	58.7	0.85
	10	1.7	35.3	4.5	58.5	0.40
	62.5	6.0	24.4	9.1	60.6	0.10

(Cu^{2+}) in oxide precursors.
[a] As percent of total metals − sum of metals = 100%.

to the presence of the OH groups (band 531.7 eV), which are formed during the preparation, mainly in the course of the reduction in hydrogen.

Similar results were obtained by Kilo et al. [33] for the Cu/ZrO_2 and $Cu/(ZrO_2 + MnO)$ catalysts. Their XPS studies showed that the surface composition deviated significantly from the bulk composition. The Cu/Zr ratio was lower at the surface and the reduction of the catalyst caused a substantial decrease in the relative surface concentration of Cu. The depletion of the surface in Cu was observed also by Strohmeier et al. [34] for Cu/Al_2O_3, and Garbassi and Petrini [35] for Cu/ZnO.

XPS data indicate that for the copper catalysts the ratio (M_{surf}/M_{av}) increases with an increase in the Cu content whereas for the catalysts containing Ag and Au a reverse tendency is observed. To a considerable degree, it is an apparent effect since the XPS signal depends not only on the content of metal M, but also on its degree of dispersion. It is generally known that when the content of the supported component exceeds an approximately monolayer coverage of the support, the XPS signal arising from that component increases very slowly and quickly reaches a plateau. This effect is due to the formation of large crystallites which because of their small relative surface area, contribute insignificantly to the XPS signal. In this light, a decrease in the M_{surf}/M_{av} ratio observed for silver and gold is a result of a considerable increase in the size of the crystallites of these metals paralleling the increase of their content in the catalysts (see Table 1). In the case of copper, the respective increase in the size of the Cu crystallites is considerably smaller, which causes only insignificant decrease of the XPS signal. Since at the same time the magnitude of this signal increases with the increase in the Cu content, the sum of these two tendencies results in a small increase in the M_{surf}/M_{av} ratio observed.

3.4. Catalytic activity of the investigated systems

Under the conditions of the catalytic tests carried out the only products of the CO_2 hydrogenation were methanol, water and carbon monoxide, therefore the hydrogenation proceeded according to two parallel reactions [7]:

$$CO_2 + 3H_2 \rightarrow CH_3OH + H_2O, \quad \Delta H_{298.50\,bar} = -40.9\,kJ/mol \tag{6}$$

$$CO_2 + H_2 \rightarrow CO + H_2O, \quad \Delta H_{298.50\,bar} = +49.8\,kJ/mol \tag{7}$$

Total conversion of CO_2 oscillated between 1 and 20% depending on the temperature and the activity of the catalysts. The selectivity to methanol decreased with increasing temperature, which was related to the increase of the participation of the endothermic reaction (7).

Fig. 9 shows the dependence between the space–time yield (STY) of methanol and temperature for the copper catalysts of a varied Cu content. The broken line marks the yield corresponding to the thermodynamic equilibrium calculated according to Skrzypek et al. [36]. A similar shape of the dependence of STY on the temperature was observed for the catalysts containing Ag and Au, but these catalysts were by far less active when compared with the copper catalysts. The yield of methanol for all investigated catalysts is compared in Table 4 for the temperature of 493 K. In the same table, the respective magnitudes of the CO_2 conversions, as well as selectivities of the hydrogenation toward methanol are given.

As our data contained in Table 4 clearly show that the copper catalysts exhibit a particularly high activity in the synthesis of methanol from CO_2. The yield of the methanol formation decrease in the series:

$$Cu \gg Au \cong Ag \tag{8}$$

but differences between the catalysts containing gold and silver are by far smaller than the differences between the copper catalysts and the remaining systems.

In contrast, the selectivity to methanol at a small conversion (1–2%) slightly increases in the series:

$$Au > Ag > Cu \tag{9}$$

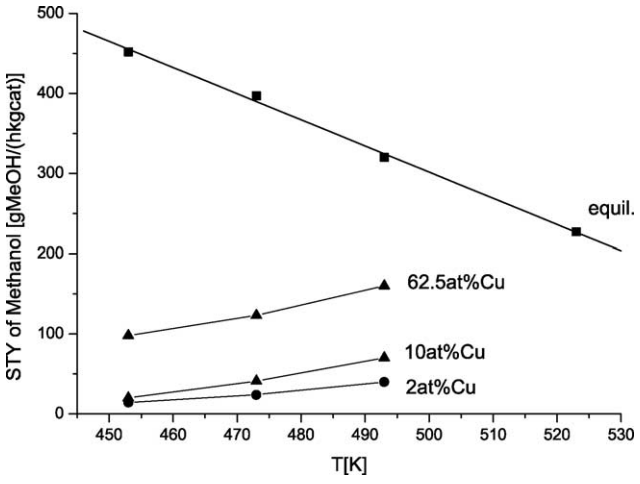

Fig. 9. Space–time yield of methanol as a function of temperature for the catalysts Cu/(3ZnO·ZrO_2) with different Cu loadings. Conditions of experiments: p = 8 MPa, GHSV = 3300 h^{-1}, H_2/CO_2 = 3.

Comparison of the rates of the methanol formation calculated per 1 mol of the metal (molar activity) shows that they decrease very quickly with the increasing metal content. There is no doubt that one of the causes of this tendency is an increase in the size of the metal grains and related decrease in the number of metal atoms exposed on the surface. To analyse if this is a sole cause of the observed decrease in the molar catalytic activity of the metal, TOF value for reaction (6) was given in the last column of Table 4. Sizes of metallic grains given in Table 1 were used in the calculations and the following surface population densities were assumed:

- 1.47×10^{19} at Cu/m^2 for Cu, which corresponds to an equal participation of (1 0 0), (1 1 0) and (1 1 1) planes in the copper crystallites. This value has been used by many authors, e.g. [25,33,37];
- 1.24×10^{19} at Ag/m^2 for Ag, which corresponds to the following participation of the planes: 25% (1 0 0) + 5% (1 1 0) + 70% (1 1 1) [38];
- 1.24×10^{19} at Au/m^2 for Au with the participation of the planes: 10% (1 0 0) + 20% (1 1 0) + 70% (1 1 1) for metal grains of the diameter $\geq$4 nm [39].

TOF values are given in parentheses for the copper catalysts, calculated from the active surface of Cu as determined from the reactive adsorption of N_2O.

It is clear that the TOF values are the greatest for the copper catalysts and they decrease following relationship (8). For all catalysts, TOF decreases with an increase in the metal content. Catalyst containing 62.5 at.% Au is an exception, since an increase in TOF is observed. This can indicate that the intermetallic phase Au_3Zn has a higher catalytic activity when compared to metallic gold. A decrease in TOF with increasing metal content indicates that a decrease in the molar catalytic activity of metals towards the formation of methanol is related not only to changes in dispersion but is due to other factors which will be discussed later.

In order to compare our results with the literature data, the following available results of other authors, for the same conditions of the reaction of the synthesis of methanol from CO_2: T = 493 K or T = 523 K, p = 8 MPa, GHSV = 3300 h^{-1}, H_2/CO_2 = 3, were collected in Table 5. To recalculate the methanol yield (STY) to the given values of pressure and flow rate, it was assumed that STY is proportional to GHSV and to $p^{0.65}$. The exponent 0.65 was determined empirically from our results and from the data contained in the paper of Ushikoshi et al. [24].

In order to facilitate analysis of the above results, relationship between the catalytic activity of the catalysts at 523 K and the metal content is shown in Fig. 10 in a semi-logarithmic system. In spite of a considerable spread of the results, one can formulate several interesting conclusions. First, it is clear that our results correspond well with the literature data shown in Table 5 and in Fig. 10. Second, a general tendency is visible that the catalytic activity related to a mole of metal M decreases with an increase in the content of this metal. One of the reasons for this decrease is

Table 4
Catalytic activity of the M/(3ZnO·ZrO_2) catalysts in the CO_2 hydrogenation

M	Content of M[a] (at.%)	Conversion of CO_2 (%)	Selectivity to methanol (%)	Catalytic activity[b]			TOF × 10^3
				g MeOH/h kg cat.	μmol MeOH/h m^2 cat.	mol MeOH/h mol M	Molecules MeOH/s surf.atom M
Cu	2	2	92	40	16.4	5.72	7.64 (10.20)
	10	9	75	71	34.8	1.99	5.25 (6.38)
	62.5	21	68	181	145.0	0.67	2.43 (4.23)
Ag	2	1	80	8.4	4.6	1.21	2.65
	10	1	95	8	8.3	0.23	1.30
	62.5	2	97	15	31.3	0.08	0.70
Au	2	1	97	11	5.8	1.62	1.69
	10	2	100	19	8.9	0.61	0.42
	62.5	1.5	100	13	16.3	0.10	0.57, 0.77[c]

The values within the parentheses are determined by N_2O decomposition.
[a] As percent of total metals − sum of metals = 100%.
[b] T = 493 K, p = 8 MPa, GHSV = 3300 h^{-1}, H_2/CO_2 = 3.
[c] Calculated for a weighted average of the crystal size of Au metal and Au_3Zn phase.

Table 5
Catalytic activity of the Cu, Ag, Au based catalysts for the CO_2 hydrogenation to methanol—literature data

Catalyst	Content of metal M (at.%)	Crystal size of metal M (nm)	Rate of methanol formation[a] (mol MeOH/h mol M)		References
			T = 493 K	T = 523 K	
Cu/ZnO	56.1	19	–	0.51	[49]
Cu/ZnO	7.1	44	–	1.63	[56]
Cu/ZnO	5.2	–	–1.76	–	[16]
	30.0	–	0.28	–	[16]
Cu/ZrO_2	13.04	30.0	3.30	3.50	[14]
Cu/ZrO_2	8.9	–	2.07	3.49	[12]
Cu/ZrO_2	60.9	26	0.26[b]	–	[21]
$Cu/ZnO/ZrO_2$	57.0	–	–	0.66	[23]
$Cu/ZnO/ZrO_2$	65.7	39.3	0.50	–	[64]
$Cu/ZnO/ZrO_2$/MnO	67.5	20.5	0.7	–	[64]
$Cu/ZnO/ZrO_2$	2.0	5.0	5.7	8.34	Presented paper
	10.0	9.8	2.0	4.58	Presented paper
	62.5	13.6	0.67	1.05	Presented paper
Ag/ZrO_2 aerogel LT	7.40	7.0	1.48	2,70	[14]
Ag/ZrO_2 aerogel HT	10.7	10.0	1.05	2.08	[14]
Ag/ZrO_2	9.26	–	1.21	2.14	[12]
$Ag/ZnO/ZrO_2$	2	16	1.21	3.01	Presented paper
	10.0	24.5	0.24	0.31	Presented paper
	62.5	43.0	0.08	0.16	Presented paper
Au/ZnO	5.0	–	–	3.20	[16]
Au/ZrO_2	5.0	–	–	1.15	[16]
Au/ZnO	5.0	3.5	–	3.19	[18]
Au/ZnO	33.0	19.5	–	0.45	[18]
Au/ZrO_2	3.2	13.5	2.19	2.82	[15]
Au/ZrO_2	25.0	8.5	1.24	1.76	[15]
Au/ZrO_2	9.43	–	3.06	4.64	[12]
$Au/ZnO/ZrO_2$	2	2.5	1.60	2.66	Presented paper
	10	3.4	0.57	1.27	Presented paper
	62.5	26.0	0.10	0.21	Presented paper

[a] Recalculated to GHSV = 3300 h^{-1} and p = 8 MPa.
[b] At 473 K.

an increase in the size of the metal grains. But, as it is visible from Table 5, other factors, most probably related to the metal–support interaction, are also significant. The results quoted clearly illustrate an exceptional position of the copper containing catalysts. A synergy between the metal and the oxide components is apparent in this system. The copper catalysts exhibit an exceptionally high activity in the methanol synthesis whereas both catalysts containing silver or gold show similar activities but considerably lower from that of the copper catalysts. Results obtained by Baiker et al. [12] pointing to a very high activity of the Au/ZrO_2 catalysts deviate considerably from the remaining results. This is a surprising situation, since the preparation conditions of this catalyst were comparable with those employed by other authors and could not account for this exceptional position.

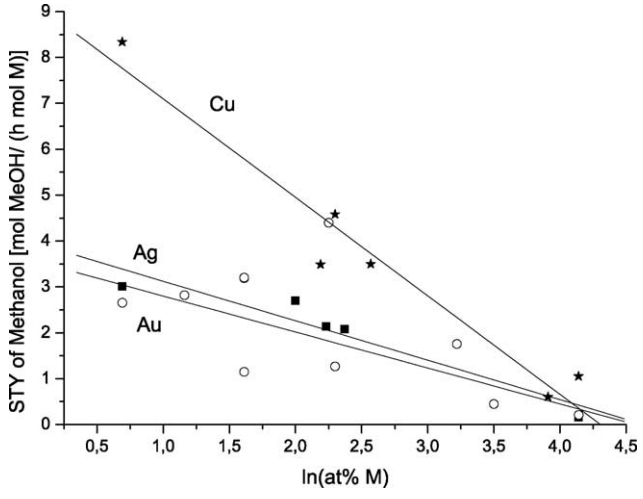

Fig. 10. Space–time yield of methanol as a function of M – metal loading at 523 K. Literature data from Table 5: p = 8 MPa; GHSV = 3300 h^{-1}; H_2/CO_2 = 3; (★) Cu; (■)) Ag; (○) Au.

Data contained in Table 5 and shown in Fig. 10 indicate that a synergy exists in both Cu/ZnO and Cu/ZrO_2 systems, as well as in the mixed catalysts containing both oxides. The mechanism of the synergy in these systems has been for years subject of investigations in many laboratories starting from classical papers of Klier [40], then of the groups of Baiker and coworkers [9,12–15], Bell and coworkers [41–44], Okamoto et al. [45], Fujita et al. [46–48], Fujitani and coworkers [49–51] and others [52–56]. In numerous studies, it has been confirmed that the stabilisation of the Cu^+ ions on the support favours the hydrogenation of CO_2 [22,23,54–56]. The Cu^+ ions can be stabilised on the surface of both

ZnO [40,45,55,56] and ZrO_2 [13,52,54] as well as of the mixed systems ZnO–ZrO_2 [22,23]. It should be expected that an analogous stabilisation effect will be considerably smaller for systems containing Ag or Au due to instability of the Ag^+ and Au^+ ions at the temperature of the catalytic reaction. This instability can be derived from values of the standard thermodynamic potential of formation of the oxides in question which are: −146, −11, +163 kJ/mol for Cu_2O, Ag_2O and Au_2O_3, respectively. In fact there is no information in the literature pointing to the presence of the above ions in catalysts containing gold or silver after the reduction and the catalytic reaction. According to Fujita et al. [46] presence of Cu^+ accelerates also the reduction of CO_2 to CO (RWGS), which would explain why the copper catalysts are less selective towards methanol when compared to the systems containing silver or gold in which the concentration of the metal ions is negligibly small.

Another aspect explaining the exceptional activity of copper is its ability to a dissociative adsorption of hydrogen. Theoretical calculations indicate that dissociation of hydrogen on metals of group IB is an activated process, contrary to the transition metals, and that atomic hydrogen does not form a permanent bond with the ideal low-index faces of large crystals of noble metals [57–59]. However, the dissociative adsorption of hydrogen was observed on powdered metals of group IB, thin films or metals laid on a support [58–61], which is related to the presence of defects of various kinds. The activation energy of the hydrogen dissociation increases in the series: Cu < Ag < Au.

Another significant factor controlling the catalytic activity is formation of a very intimate contact between the noble metal and the support, which is favoured by a high dispersion of the components. The mechanism of the catalyst's activity proposed by the Bell's group assumes existence of mixed CuZr centres which co-operate in the elementary steps of the reaction [41]. Formation of such centres in the conditions of the reaction were described recently by Fujitani and coworkers [50,51,62,63] for the Cu/ZnO system.

Next factor concerns a possibility of a change in the morphology of the metallic grains which manifests itself in varying proportions of amorphous and crystalline forms [45]. For crystallites, an increase in the proportion of high-index faces, containing steps, can occur, which is equivalent to an increase in a number of more active atoms located on edges or corners. Fujita et al. [48] showed that the dissociative adsorption of CO_2 on copper is structurally sensitive and is accelerated on faces containing steps, e.g. on the (3 1 1) plane of Cu. This favours the RWGS reaction and contributes to a decrease in the selectivity to methanol in the reaction of synthesis from CO_2.

In complex catalysts a number of factors listed above have their effect concurrently and it is difficult to relate them unequivocally to the progress of the catalytic reaction. It should be stressed that in spite of the complexity of the situation certain general tendencies are observed and that they were formulated above basing on the literature review and the present results.

4. Conclusions

1. Metal dispersion in the investigated catalysts decreases with an increase in the metal content, it depends also on the metal type and decreases in the series Cu ≅ Au > Ag.
2. Amorphous ZrO_2 and crystalline ZnO are present in all catalysts investigated which undergo segregation. Metallic copper is present mainly close to ZnO. Silver is distributed uniformly, but sizes of the Ag crystallites are considerably larger when compared to Cu. In catalysts of low gold content (≤10 at.%), Au accumulates preferentially close to amorphous ZrO_2, whereas in catalysts of high gold content, the distribution of Au is more uniform.
3. The catalytic activity of metals IB in hydrogenation of CO_2 to methanol increases with the increase of the metal dispersion.
4. The copper catalysts exhibit a particularly high catalytic activity in the methanol synthesis from CO_2. Synergy between Cu and support is apparent in this system. The molar catalytic activity and TOF decreases in the series Cu ≫ Au≅Ag whereas the selectivity to methanol varies insignificantly in the series: Au > Ag > Cu.
5. The synergy mechanism involves probably a stabilisation of the Cu^+ ions on the surface of ZnO or/and ZrO_2, which accelerates the dissociative adsorption of CO_2. For catalysts containing gold or silver the above mechanism is less effective, since the respective Ag^+ and Au^+ ions are less stable in the conditions of the reaction.

Acknowledgments

The work was financed by the State Committee for Scientific Research, KBN, under the Project No. 7 T09C 01021. The assistance of Ms. Zofia Czuła in the BET and porosity measurements is gratefully acknowledged.

References

[1] J. Haggin, Chem. Eng. News 72 (1994) 29.
[2] Proceedings of the Advances in Chemical Conversions for Mitigating Carbon Dioxide Conference, Kioto, 1997; Stud. Surf. Sci. Catal. 114 (1998).
[3] J.P. Breen, J.R.H. Ross, Catal. Today 51 (1999) 521.
[4] S. Velu, K. Suzuki, M. Okazaki, M.P. Kapoor, T. Osaki, F. Ohashi, J. Catal. 194 (2000) 373.
[5] P.J. de Wild, M.J.F.M. Verhaak, Catal. Today 60 (2000) 3.
[6] J. Skrzypek, J. Słoczyński, S. Ledakowicz, Metanol Synthesis, Polish Scientific Publishers (PWN), Warszawa, 1994.
[7] J.B. Hansen, Handbook of Heterogenous Catalysis, vol. 4, VCH–Wiley, Weinheim, 1997p. 1856.
[8] Y.M.Q. Sun, D. Wu, W.-H. Fan, Y.-L. Zhang, J.-F. Deng, Appl. Catal. A: Gen. 171 (1998) 45.

[9] J. Wambach, A. Baiker, A. Wokaun, Phys. Chem. Chem. Phys. 1 (1999) 5071.
[10] E.E. Ortelli, J. Wambach, A. Wokaun, Appl. Catal. A: Gen. 216 (2000) 227.
[11] J.C. Frost, Nature 334 (1988) 577.
[12] A. Baiker, M. Kilo, M. Maciejewski, S. Menzi, A. Wokaun, in: Proceedings of the 10th International Congress on Catalysis, Budapest, 1992, p. 208.
[13] C. Fröhlich, R.A. Köppel, A. Baiker, M. Kilo, A. Wokaun, Appl. Catal. A: Gen. 106 (1993) 275.
[14] R.A. Köppel, C. Stöcker, A. Baiker, J. Catal. 179 (1998) 515.
[15] R.A. Köppel, A. Baiker, Ch. Schied, A. Wokaun, J. Chem. Soc., Faraday Trans. 87 (1991) 2821.
[16] H. Sakurai, S. Tsubota, M. Haruta, Appl. Catal. A: Gen. 102 (1993) 125.
[17] H. Sakurai, M. Haruta, Appl. Catal. A: Gen. 127 (1995) 93.
[18] H. Sakurai, M. Haruta, Catal. Today 29 (1996) 361.
[19] T. Tabakowa, V. Idakiev, D. Andreeva, I. Mitov, Appl. Catal. A: Gen. 202 (2000) 91.
[20] S. Sakahara, K. Yajima, R. Belosludov, S. Takami, M. Kubo, A. Miyamoto, Appl. Surf. Sci. 189 (2002) 253.
[21] Y. Nitta, O. Suwata, Y. Ikeda, Y. Okamoto, T. Imanaka, Catal. Lett. 26 (1994) 345.
[22] M. Saito, T. Fujitani, I. Takahara, T. Watanabe, M. Takeuchi, Y. Kanai, K. Moriya, T. Kakumoto, Energ. Convers. Manage. 36 (1995) 577.
[23] M. Saito, T. Fujitani, M. Takeuchi, T. Watanabe, Appl. Catal. A: Gen. 138 (1996) 311.
[24] K. Ushikoshi, K. Mori, T. Watanabe, M. Takeuchi, M. Saito, Stud. Surf. Sci. Catal. 114 (1998) 357.
[25] J. Skrzypek, J. Słoczyński, S. Ledakowicz, Metanol Synthesis, Polish Scientific Publishers (PWN), Warszawa, 1994, p. 45 and reference therein.
[26] J. Szajman, J. Liesegang, J.G. Jenkin, R.C.G. Leckey, J. Electron Spectrosc. Relat. Phenom. 23 (1981) 97.
[27] D.R. Penn, J. Electron Spectrosc. 9 (1976) 29.
[28] 2nd ed. D. Briggs, M.P. Seah (Eds.), Auger and X-Ray Photoelectron Spectroscopy, vol. I, Wiley, New York, 1990, p. 635(Appendix 6).
[29] S.E. Wanke, P.C. Flynn, Catal. Rev. Sci. Eng. 12 (1976) 93.
[30] J.A. Bett, K. Kinoshita, P. Stonehart, J. Catal. 35 (1974) 307.
[31] K. Hisatsune, Y. Takuma, Y. Tanaka, K. Udoh, T. Morimura, M. Hasaka, Solid State Commun. 106 (1998) 509.
[32] R.T.K. Baker, J. Catal. 78 (1982) 473.
[33] M. Kilo, J. Weigel, A. Wokaun, R.A. Koeppel, A. Stoeckli, A. Baiker, J. Mol. Catal. A: Chem. 126 (1997) 169.
[34] B.R. Strohmeier, D.E. Leyden, R. Scott Field, D.M. Hercules, J. Catal. 94 (1985) 514.
[35] F. Garbassi, G. Petrini, J. Catal. 90 (1984) 113.
[36] J. Skrzypek, M. Lachowska, D. Serafin, Chem. Eng. Sci. 45 (1990) 89.
[37] R.J. Matyi, L.H. Schwartz, J.B. Butt, Catal. Rev. Sci. Eng. 29 (1987) 41.
[38] B.E. Sundquist, Acta Met. 12 (1964) 67.
[39] S. Schimpf, M. Lucas, Ch. Mohr, U. Rodemerck, A. Brückner, J. Radnik, H. Hofmeister, P. Claus, Catal. Today 72 (2002) 63.
[40] K. Klier, Adv. Catal. 31 (1982) 243.
[41] I.A. Fisher, A.T. Bell, J. Catal. 172 (1997) 222.
[42] I.A. Fisher, A.T. Bell, J. Catal. 178 (1998) 153.
[43] I.A. Fisher, A.T. Bell, J. Catal. 184 (1999) 357.
[44] K.-D. Jung, A.T. Bell, J. Catal. 193 (2000) 207.
[45] Y. Okamoto, K. Fukino, T. Imanaka, S. Teraniski, J. Phys. Chem. 87 (1983) 3747.
[46] S.-I. Fujita, M. Usui, N. Takezawa, J. Catal. 134 (1992) 220.
[47] S.-I. Fujita, M. Usui, H. Ito, N. Takezawa, J. Catal. 157 (1995) 403.
[48] S.-I. Fujita, S. Moribe, Y. Kanamori, M. Kakudate, N. Takezawa, Appl. Catal. A: Gen. 207 (2001) 121.
[49] T. Fujitani, J. Nakamura, Catal. Lett. 56 (1998) 119.
[50] T. Fujitani, J. Nakamura, Appl. Catal. A: Gen. 191 (2000) 111.
[51] Y. Choi, K. Futagami, T. Fujitani, J. Nakamura, Appl. Catal. A: Gen. 208 (2001) 163.
[52] J. Liu, J. Shi, D. He, Q. Zhang, X. Wu, Yu. Liang, Q. Zhu, Appl. Catal. A: Gen. 218 (2001) 113.
[53] H.Y. Chen, S.P. Lau, L. Chen, J. Lin, C.H.A. Huan, K.L. Tan, J.S. Pan, Appl. Surf. Sci. 152 (1999) 193.
[54] Y.W. Suh, S.-H. Moon, H.-K. Rhee, Catal. Today 63 (2000) 447.
[55] J. Toyir, P.R. de la Piscina, J.L.G. Fierro, N. Homs, Appl. Catal. B: Environ. 29 (2001) 207.
[56] J. Toyir, P.R. de la Piscina, J.L.G. Fierro, N. Homs, Appl. Catal. B: Environ. 34 (2001) 255.
[57] B. Hammer, J.K. Norskov, Nature 376 (1995) 238.
[58] R. Duś, Progr. Surf. Sci. 42 (1993) 231.
[59] R. Duś, E. Nowicka, Progr. Surf. Sci. 74 (2003) 39.
[60] M. Okada, M. Nakamura, K. Moritani, T. Kasai, Surf. Sci. 523 (2003) 218.
[61] M.J. Sandoval, A.T. Bell, J. Catal. 144 (1993) 227.
[62] T. Fujitani, I. Nakamura, T. Uchijima, J. Nakamura, Surf. Sci. 383 (1997) 285.
[63] I. Nakamura, T. Fujitani, T. Uchijima, J. Nakamura, Surf. Sci. 400 (1998) 387.
[64] J. Słoczyński, R. Grabowski, A. Kozłowska, P. Olszewski, M. Lachowska, J. Skrzypek, J. Stoch, Appl. Catal. A: Gen. 249 (2003) 129.